Neuron
Article

Misfolded Mutant SOD1 Directly Inhibits VDAC1 Conductance in a Mouse Model of Inherited ALS

Adrian Israelson,[1] Nir Arbel,[2] Sandrine Da Cruz,[1] Hristelina Ilieva,[1] Koji Yamanaka,[3] Varda Shoshan-Barmatz,[2] and Don W. Cleveland[1,*]
[1]Ludwig Institute for Cancer Research and Departments of Cellular and Molecular Medicine and Neurosciences, University of California at San Diego, La Jolla, CA 92093-0670, USA
[2]Department of Life Sciences and the National Institute for Biotechnology in the Negev, Ben-Gurion University of the Negev, Beer-Sheva 84105, Israel
[3]Laboratory of Motor Neuron Diseases, RIKEN Brain Science Institute, 2-1 Hirosawa, Wako-shi, Saitama 351-0198, Japan
*Correspondence: dcleveland@ucsd.edu
DOI 10.1016/j.neuron.2010.07.019

SUMMARY

Mutations in superoxide dismutase (SOD1) cause amyotrophic lateral sclerosis (ALS), a neurodegenerative disease characterized by loss of motor neurons. With conformation-specific antibodies, we now demonstrate that misfolded mutant SOD1 binds directly to the voltage-dependent anion channel (VDAC1), an integral membrane protein imbedded in the outer mitochondrial membrane. This interaction is found on isolated spinal cord mitochondria and can be reconstituted with purified components in vitro. ADP passage through the outer membrane is diminished in spinal mitochondria from mutant SOD1-expressing ALS rats. Direct binding of mutant SOD1 to VDAC1 inhibits conductance of individual channels when reconstituted in a lipid bilayer. Reduction of VDAC1 activity with targeted gene disruption is shown to diminish survival by accelerating onset of fatal paralysis in mice expressing the ALS-causing mutation $SOD1^{G37R}$. Taken together, our results establish a direct link between misfolded mutant SOD1 and mitochondrial dysfunction in this form of inherited ALS.

INTRODUCTION

Amyotrophic lateral sclerosis (ALS) is a progressive adult-onset neurodegenerative disorder characterized by the selective loss of upper and lower motor neurons in the brain and spinal cord (Cleveland and Rothstein, 2001). The typical age of onset is between 50 to 60 years, followed by paralysis and ultimately death within 2–5 years after onset (Mulder et al., 1986). Most instances of ALS are sporadic lacking any apparent genetic linkage, but 10% are inherited in a dominant manner. Twenty percent of these familial cases have been attributed to mutations in the gene encoding cytoplasmic Cu/Zn superoxide dismutase (SOD1) (Rosen et al., 1993). Although multiple hypotheses have been proposed to explain mutant SOD1-mediated toxicity (Ilieva et al., 2009), the exact mechanism(s) responsible for motor neuron degeneration remains unsettled.

Mitochondrial dysfunction has been proposed to contribute to disease pathogenesis. Histopathological observations of disturbed mitochondrial structure have been reported in muscle of both sporadic and familial ALS patients (Hirano et al., 1984a, 1984b; Sasaki and Iwata, 1996, 2007) and in mutant SOD1 mouse models expressing dismutase active (Dal Canto and Gurney, 1994; Higgins et al., 2003; Kong and Xu, 1998; Wong et al., 1995), but not inactive mutants (Bruijn et al., 1997). Moreover, functionality of mitochondria has been reported to be affected in spinal cord and skeletal muscles of human sporadic ALS or familial ALS patients (Dupuis et al., 2003; Echaniz-Laguna et al., 2002; Vielhaber et al., 1999; Wiedemann et al., 2002), as well as in some ALS mouse models (Damiano et al., 2006; Mattiazzi et al., 2002; Nguyen et al., 2009).

A proportion of the predominantly cytosolic SOD1 has been reported to localize to mitochondria in certain contexts. In both rodent models and patient samples, mutant SOD1 is present in fractions enriched for mitochondria derived from affected, but not unaffected, tissues (Bergemalm et al., 2006; Deng et al., 2006; Liu et al., 2004; Mattiazzi et al., 2002; Vande Velde et al., 2008; Vijayvergiya et al., 2005) and a clear temporal correlation between mitochondrial association and disease progression was shown for multiple mutant SOD1s (Liu et al., 2004). Purification of mitochondria, including floatation steps that eliminate protein only aggregates, coupled with protease accessibility has demonstrated mutant SOD1 deposition on the cytoplasmic-facing surface of spinal cord mitochondria (Liu et al., 2004; Vande Velde et al., 2008). Sensitivity to proteolysis and immunoprecipitation with an antibody specific for misfolded SOD1 further indicated that misfolded forms of dismutase active and inactive SOD1 are deposited onto the cytoplasmic face of the outer membrane of spinal cord mitochondria (Vande Velde et al., 2008). This is accompanied by altered accumulated levels of a few mitochondrial proteins, reduced import of multiple mitochondrial proteins, and reduced complex I activity (T. Miller, C. Vande Velde, and D.W.C., unpublished data).

Oxidative phosphorylation requires the transport of metabolites, including ADP, ATP, and inorganic phosphate across both mitochondrial membranes. Located in the outer mitochondrial membrane, the voltage-dependent anion channel (VDAC),

known as mitochondrial porin, assumes a crucial position in the cell, controlling metabolic cross-talk between the mitochondrion and the rest of the cell, thus regulating the metabolic and energetic functions of mitochondria (Shoshan-Barmatz et al., 2006, 2008). Of the three VDAC isoforms (VDAC1–3), VDAC1 is the most abundant in most cells. VDAC1 is a primary contributor to ATP/ADP flux across the outer mitochondrial membrane (Colombini, 2004; Lemasters and Holmuhamedov, 2006). Initially named somewhat misleadingly as a channel for anions, it is also responsible for import/export of Ca^{2+} (Gincel et al., 2001) and other cations (Benz, 1994; Colombini, 2004), adenine nucleotides (Rostovtseva and Colombini, 1997; Rostovtseva and Bezrukov, 1998) and other metabolites (Hodge and Colombini, 1997). Indeed, it has been demonstrated that silencing VDAC1 expression in a cultured cell line using shRNA resulted in reduced ATP production and a decrease in cell growth (Abu-Hamad et al., 2006).

VDAC1 is also a key player in mitochondria-mediated apoptosis. VDAC1 has been implicated in apoptotic-relevant events, due to serving as the target for members of the pro- and anti-apoptotic Bcl2-family of proteins (Arbel and Shoshan-Barmatz, 2010; Shimizu et al., 1999) and due to its function in the release of apoptotic proteins from the intermitochondrial membrane space (Abu-Hamad et al., 2009; Shoshan-Barmatz et al., 2006, 2008; Tajeddine et al., 2008). VDAC1 has also been implicated in Parkinson's disease as a direct target for Parkin-mediated poly-ubiquitylation and mitophagy (Geisler et al., 2010).

Starting from recognition that a proportion of misfolded, mutant SOD1 is bound to the cytoplasmic face of the outer membrane of mitochondria in affected tissues (Liu et al., 2004; Rakhit et al., 2007; Vande Velde et al., 2008), we now identify damage to spinal cord mitochondria to arise through direct binding of misfolded SOD1 onto the cytoplasmic-facing domain of VDAC1, thereby inhibiting its conductance.

RESULTS

Mutant SOD1 and VDAC1 Interact In Vivo in Spinal Cord of Transgenic SOD1 Rats

To investigate potential interactions between mutant SOD1 and VDAC1, mitochondria from rats expressing wild-type human SOD1 ($hSOD1^{wt}$) or either of two different ALS-linked SOD1 mutants, a dismutase active $hSOD1^{G93A}$ and a dismutase inactive $hSOD1^{H46R}$, were highly purified by repeated centrifugation steps (summarized in Figure 1A) including a final density gradient flotation step to eliminate any contaminating protein only aggregates (proteins sediment downward in these conditions because of their higher density), as previously described (Vande Velde et al., 2008). Immunoblotting of immunoprecipitates generated after addition of an SOD1 antibody to solubilized mitochondrial lysates revealed that a proportion of VDAC1 was coprecipitated with dismutase active and inactive mutant SOD1, but not wild-type SOD1 (Figure 1B). Parallel immunoprecipitations with a VDAC1 antibody confirmed coprecipitation of both $hSOD1^{G93A}$ and $hSOD1^{H46R}$ with VDAC1 (Figure 1D). Binding to VDAC1 was a property only of spinal cord mitochondria, as no association of mutant SOD1 was seen with purified brain mitochondria from the same animals using immunoprecipitation with SOD1 (Figure 1C) or VDAC1 (Figure 1E) antibodies. This latter finding is consistent with prior efforts that had demonstrated that mutant SOD1 associates with the cytoplasmic face of the outer membrane of mitochondria in spinal cord, but not other tissue types (Liu et al., 2004; Vande Velde et al., 2008). Moreover, mutant SOD1 binding to VDAC1 is inversely correlated with the level of hexokinase-I, a known partner that binds to VDAC1 exposed on the cytoplasmic mitochondrial surface (Abu-Hamad et al., 2008; Azoulay-Zohar et al., 2004; Zaid et al., 2005), with hexokinase accumulating to much higher level in brain than spinal cord mitochondria (Figure 1F).

Misfolded Mutant SOD1 Specifically Interacts with VDAC1 In Vivo in Spinal Cord of Transgenic SOD1 Rats

To test the nature of the interaction between mutant SOD1 and VDAC1, immunoprecipitation was performed with a SOD1 antibody that recognizes a "disease-specific epitope" (DSE) that is unavailable on correctly folded SOD1 (Cashman and Caughey, 2004; Paramithiotis et al., 2003; Urushitani et al., 2007), but is present on misfolded mutant SOD1s in inherited ALS (Rakhit et al., 2007). Using one such antibody (DSE2), age-dependent deposition of mutant SOD1 onto the cytoplasmic face of spinal cord mitochondria has been shown to reflect association of misfolded SOD1 (Vande Velde et al., 2008). We exploited this antibody to examine if the SOD1 associated with VDAC1 is bound through misfolded SOD1. Liver, brain, and spinal cord cytosolic and mitochondrial fractions purified from symptomatic rats expressing mutant $hSOD1^{G93A}$ were immunoprecipitated (see schematic in Figure 2A) with the DSE2 antibody, which recognizes an epitope in the electrostatic loop of hSOD1 (between residues 125–142) that is buried in normally folded SOD1. Misfolded mutant $SOD1^{G93A}$ was not detectable in the soluble fraction of any tissue, but was immunoprecipitated from the spinal cord, but not liver or brain, mitochondrial fractions (Figure 2B).

Solubilized spinal cord mitochondria purified from presymptomatic and symptomatic rats expressing either of two different SOD1 mutants, dismutase active $hSOD1^{G93A}$ and dismutase inactive $hSOD1^{H46R}$, as well as $hSOD1^{wt}$ were immunoprecipitated with the DSE2 antibody and coimmunoprecipitated components identified by immunoblotting. An age-dependent increase in misfolded SOD1 was seen for both mutants, with a significantly higher proportion of the dismutase inactive $SOD1^{H46R}$ in a misfolded conformation. In samples from symptomatic animals, VDAC1 coprecipitated together with the misfolded mutant SOD1, as revealed by immunoblotting of immunoprecipitates (Figure 2C). This association was selective for VDAC1, as misfolded mutant SOD1 did not coimmunoprecipitate with any of three other mitochondrial proteins examined (Figure 2C), including two additional outer mitochondrial membrane proteins with domains facing the cytoplasm: TOM40, the 40 kDa component of *t*ransport across the *o*uter *m*embrane (TOM) complex mediating all protein import from the cytoplasm to the mitochondria, and VDAC2, a second voltage-dependent anion channel isoform that has been estimated to represent 7% (kidney) to 25% (brain) of accumulated VDAC (Yamamoto

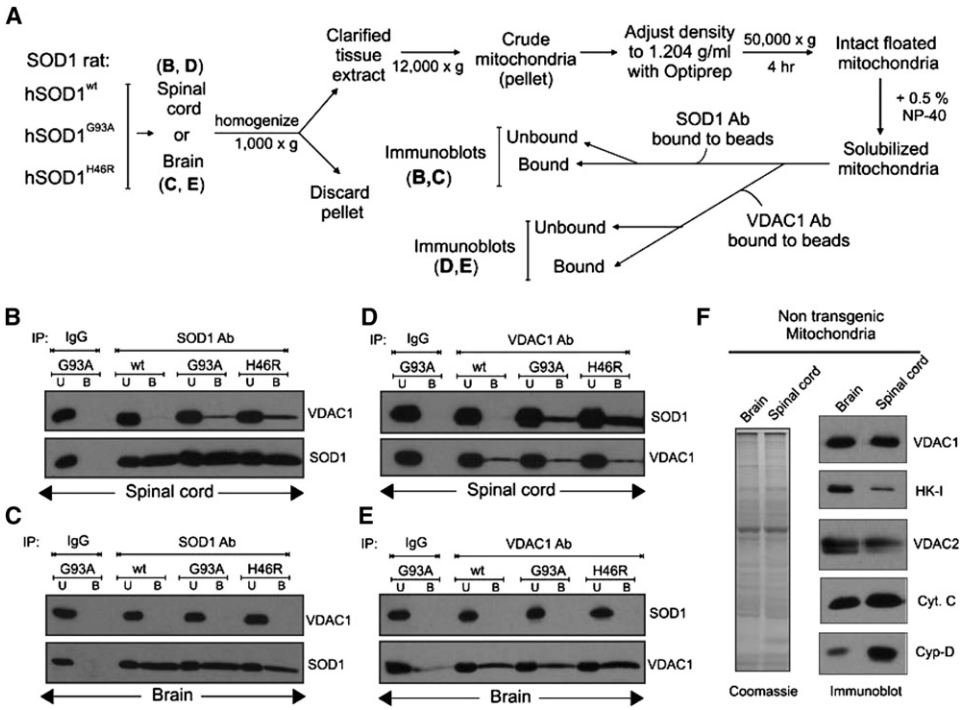

Figure 1. A Complex Containing Mutant SOD1 and VDAC1 from Spinal Cord Mitochondria

(A) Schematic outlining the different purification steps used. Floated isolated mitochondria from (B and D) hSOD1^{wt}, hSOD1^{G93A}, and hSOD1^{H46R} rat spinal cords or (C and E) brain were immunoprecipitated with (B and C) an SOD1 antibody or (D and E) VDAC1 antibody.

(B) Immunoblot of the SOD1 immunoprecipitates using VDAC1 antibody indicates that mutant SOD1 proteins hSOD^{G93A} and hSOD1^{H46R} coprecipitate VDAC1 (top). SOD1 immunoprecipitation was confirmed by reprobing the membrane with anti-SOD1 antibody (bottom).

(C) Immunoblots of SOD1 immunoprecipitates as in (B) except with brain mitochondria.

(D) Immunoprecipitation using VDAC1 antibody immunoblotted with SOD1 antibody (top). The membrane was then reprobed for VDAC1 (bottom).

(E) Immunoblots of VDAC1 immunoprecipitates as in (D), except with brain mitochondria. Abbreviations: U, unbound fraction (20%); B, bound fraction.

(F) Reduced hexokinase-I levels in spinal cord mitochondria. Polyacrylamide gel analysis of extracts of floated brain and spinal cord mitochondria. (Left) Coomassie stain; (right) immunoblot for VDAC1, hexokinase I (HK-I), VDAC2, cytochrome c (Cyt. C), and cyclophilin D (Cyp-D).

et al., 2006). It also did not coprecipitate cyclophilin-D, an important component of the permeability transition pore.

Furthermore, in order to determine which cells accumulate the misfolded form of SOD1, we performed immunostaining using the DSE2 antibody. Spinal cords from loxSOD1^{G37R} mice at different stages of the disease were subjected to immunostaining with DSE2 antibody (Figure 2D). The accumulation of misfolded SOD1 dramatically increased with disease progression. Although little accumulation of misfolded SOD1 is found by disease onset, it was preferentially found within motor neurons. During disease progression, a dramatic increase of misfolded SOD1 was apparently accumulated in other cells as well and probably also extracellularly. Throughout disease a proportion of the misfolded SOD1 was colocalized with mitochondria of motor neurons and other cells, starting at onset and increasing with disease progression (Figure 2D).

Binding of Mutant SOD1 Directly Inhibits VDAC1 Channel Conductance

To test if binding of mutant SOD1 affects VDAC1 function, VDAC1 was purified from spinal cords of nontransgenic rats (Figure 3A) and reconstituted into a planar lipid bilayer (Figure 3A) using conditions previously demonstrated to yield polarized VDAC1 membrane insertion such that the VDAC1 surface exposed on the *cis* side is the surface exposed to the cytosol when inserted into the mitochondrial outer membrane (Azoulay-Zohar et al., 2004; Israelson et al., 2005; Arbel and Shoshan-Barmatz, 2010). Activity of individual channels was measured as a function of time by the ions passing across the bilayer in response to an applied voltage gradient. This revealed that in the absence of SOD1, VDAC1 was stably in a fully open state (4 nS at 1 M KCl [Shoshan-Barmatz et al., 2006]) and remained so for extended periods.

Mutant SOD1 proteins hSOD1^{G93A}, hSOD1^{G85R}, as well as hSOD1^{wt}, were expressed using baculovirus and purified (Figure 3C; Hayward et al., 2002). Wild-type SOD1, even at the highest added concentration (8 μg/ml), had no effect on VDAC1 conductance when added on either *cis* or *trans* sides of the membrane (Figures 3E and 3I). However, addition of purified recombinant hSOD1^{G93A} or hSOD1^{G85R} (Figure 3C) substantially reduced VDAC1 channel conductance (Figures 3F and 3G). Both mutant SOD1s modified VDAC1 conductance only when added to the *cis* side (Figures 3F and 3G), but not the *trans* side (Figures 3J and 3K) of the bilayer, indicating that mutant SOD1 interacts

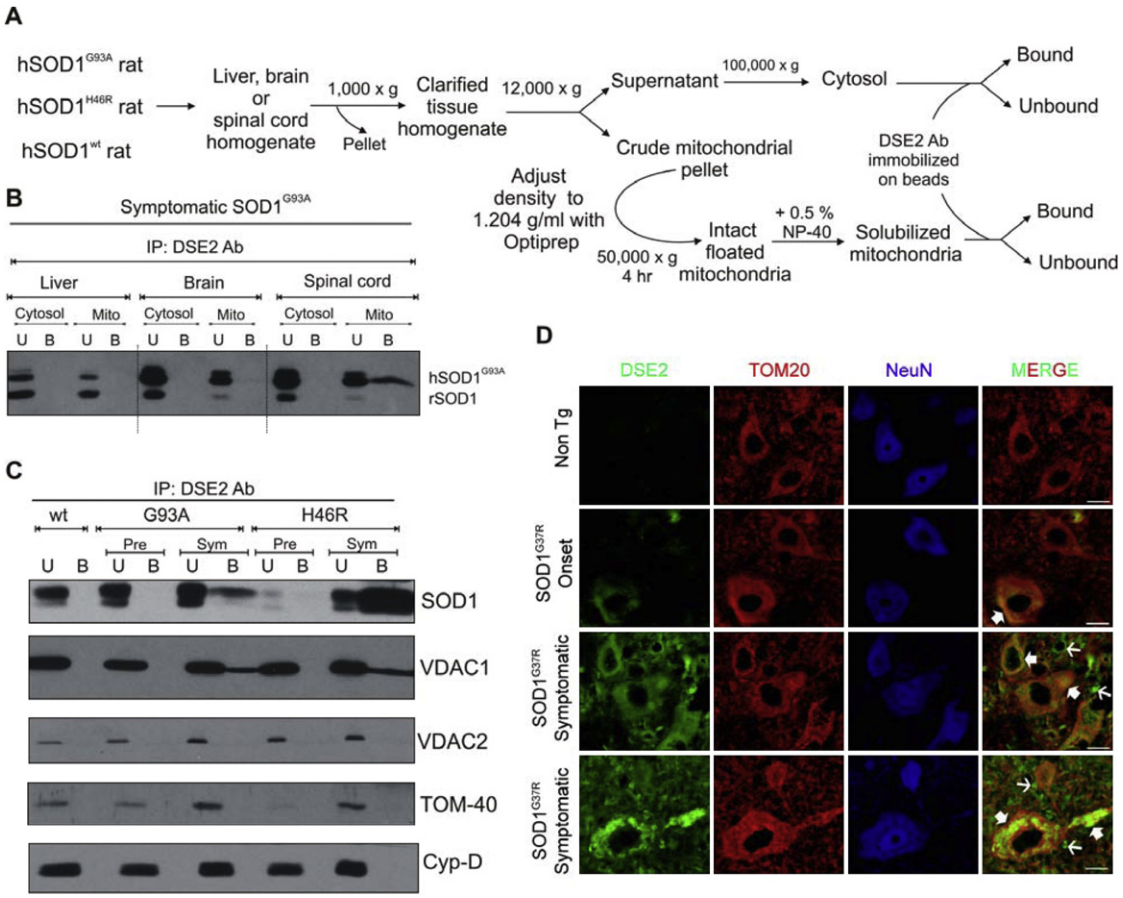

Figure 2. The Misfolded Mutant SOD1 Specifically Coprecipitates with VDAC1 in Spinal Cord Mitochondria

(A) Schematic showing the isolation of cytosolic and mitochondrial fractions.

(B) Liver, brain, and spinal cord cytosolic, and mitochondrial fractions were purified from symptomatic rats expressing hSOD1^{G93A} and the fractions were subjected to immunoprecipitation using DSE2 (3H1), a monoclonal antibody only recognizing misfolded SOD1 (Vande Velde et al., 2008). The immunoprecipitates were immunoblotted using an SOD1 antibody.

(C) Isolated floated mitochondria from hSOD1^{wt}, hSOD1^{G93A}, and hSOD1^{H46R} rat spinal cords (from presymptomatic and symptomatic animals) were immunoprecipitated with DSE2 (3H1), and the immunoprecipitates were immunoblotted using VDAC1, VDAC2, TOM-40, and cyclophilin-D antibodies. SOD1 immunoprecipitation was confirmed by reprobing the membrane with an SOD1 antibody (top).

(D) Immunohistochemical detection of misfolded SOD1 using DSE2 antibody shows that misfolded SOD1 (green) colocalizes with TOM20 (red), a mitochondrial outer membrane protein in a subset of spinal cord neurons assessed using NeuN (blue), a neuronal marker as highlighted by filled arrows. DSE2 positive staining can be detected in some neurons at onset and significantly increases with the appearance of disease symptoms.

Of note DSE2 staining is not restricted to neuronal mitochondria but is also detected in nonneuronal cells and the extracellular space as shown with thin arrows. No DSE2 staining was detected in neurons of 1 year old nontransgenic control mice (Non Tg). Scale bar: 10 μm. Abbreviation: U, unbound fraction (20%); B, bound fraction; Pre, presymptomatic; Sym, symptomatic.

with what would correspond to the cytosolic face of VDAC1 inserted into the outer mitochondrial membrane. Use of multichannel recordings revealed that not only did mutant SOD1 significantly lower the maximum voltage gated conductance of individual channels, it also provoked a stable, reduced level of VDAC1 conductance at all applied voltages (Figures 3L–3N). In order to determine if this interaction is specific for mutant SOD1, the effect of another aggregating protein (α-synuclein) was tested on bilayers containing reconstituted VDAC1. Even when added to levels 25 times greater than an amount of mutant SOD1 that markedly affected VDAC1 conductance (Figures 3F and 3G), neither wild-type nor mutant α-synuclein affected VDAC1 channel activity at any voltage (Figure 1S).

ADP Transport across the Outer Mitochondrial Membrane Is Reduced in Spinal Cords of Mutant SOD1 Rats

Since both dismutase active and inactive SOD1 mutant proteins reduced VDAC1 channel conductance for K^+ and Cl^- (Figure 3), we next tested whether mitochondrial conductance across the outer mitochondrial membrane was affected in animals chronically expressing mutant SOD1. To do this, we examined the uptake into mitochondria of adenine nucleotides (Figure 4A) which are known to be transported by VDAC1 (Lemasters and Holmuhamedov, 2006; Rostovtseva and Colombini, 1997). Freshly isolated spinal cord and liver mitochondria from SOD1^{G93A} rats were incubated (for 1 min)

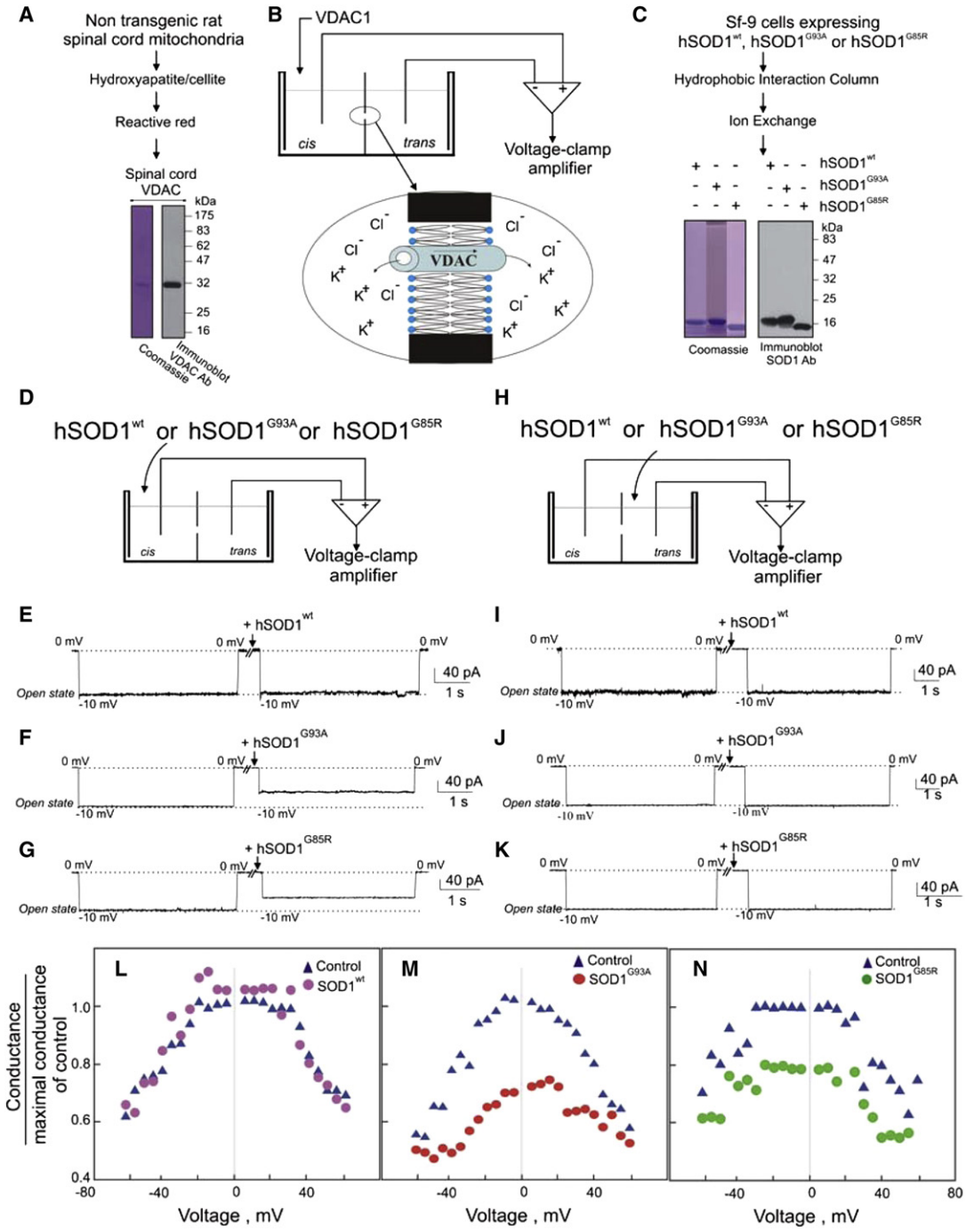

Figure 3. Mutant, but Not Wild-Type, SOD1 Interacts with Bilayer-Reconstituted VDAC1 to Reduce Its Channel Conductance

(A) Coomassie Blue staining and immunoblot of purified VDAC1 purified from rat spinal cord.

(B) Schematic presentation showing the planar lipid bilayer reconstitution and channel conductance assay system. Purified spinal cord VDAC1 was reconstituted into a planar lipid bilayer, and channel currents through VDAC1 were recorded.

(C) Coomassie Blue staining and immunoblot of purified recombinant hSOD1^{wt}, hSOD1^{G93A}, and hSOD1^{G85R} expressed in insect cells using baculovirus.

(D–G) Currents through VDAC1 in response to a voltage step from 0 to −10 mV were recorded before and 2 min after the addition (to 2 μg/ml final) of purified recombinant (E) hSOD1^{wt}, (F) hSOD1^{G93A}, or (G) hSOD1^{G85R} to the *cis* side of the bilayer.

(H–K) Currents through VDAC1 as in (D)–(G), except after SOD1 addition to the *trans* side of the bilayer. The dotted lines indicate current levels in the maximal and zero conductance states. These examples are representative of the results from 3–4 independent reconstitution experiments.

(L–N) Mutant SOD1 effect on VDAC1 channel activity at different voltages. Average steady-state conductance of VDAC1 before and after addition of (L) hSOD1^{wt}, (M) hSOD1^{G93A}, or (N) hSOD1^{G85R}, determined as a function of voltage with a multichannel recording.

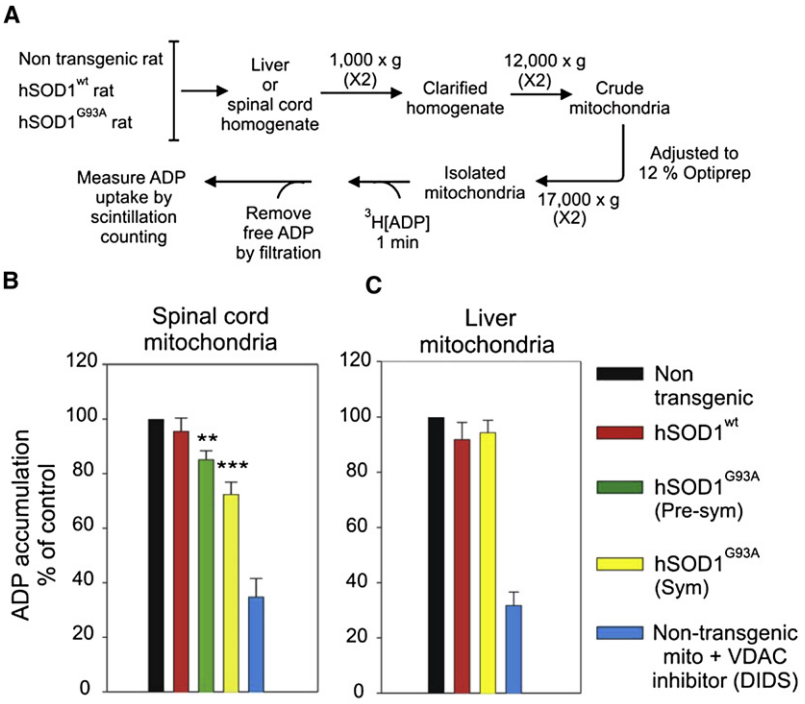

Figure 4. ADP Transport across the Outer Mitochondrial Membrane Is Reduced in Mitochondria from Spinal Cord of SOD1^{G93A} ALS Rats

(A) Schematic presentation of method for measuring ADP accumulation into isolated mitochondria as measured using radio-labeled [^{3}H]ADP.

(B and C) Mitochondria were isolated from (B) spinal cord and (C) liver of nontransgenic, hSOD1^{wt}, hSOD1^{G93A} presymptomatic, and hSOD1^{G93A} symptomatic rats. Student's t test was used and $p < 0.001$ (marked by three asterisks) and $p < 0.01$ (marked by two asterisks) were considered statistically significant. Values represent the means ± SEM of three to four independent experiments.

with radio-labeled [^{3}H]ADP and the amount of imported ADP was measured by scintillation counting after rapid filtration to remove the unincorporated ADP. Coincubation with 1 mM of the VDAC1 inhibitor DIDS (4, 4′-diisothiocyanostilbene-2, 2′-disulfonic acid) demonstrated that ~2/3 of the ADP uptake was through VDAC1 (Figures 4B and 4C). Compared to mitochondria from non-transgenic animals, uptake of ADP by spinal cord mitochondria from SOD1 mutant expressing animals was selectively and progressively inhibited, yielding ~40% inhibition of VDAC1-dependent uptake (~25% overall inhibition of ADP uptake) by a symptomatic stage (Figure 4B). Inhibition of ADP uptake was selective to spinal mitochondria as liver mitochondria from the same hSOD1^{G93A} animals retained normal ADP import at all ages examined (Figure 4C).

Mutant SOD1 Binding to Mitochondria In Vitro Diminishes ADP but Not Ca^{2+} Uptake

To test if inhibition of ADP import seen in spinal cord mitochondria from mutant SOD1 animals could be generated solely from mutant SOD1 binding to the cytoplasmic face of those mitochondria, purified recombinant SOD1 proteins (hSOD1^{wt}, hSOD1^{G93A}, and hSOD1^{G85R}) (Figure 3C) were added to mitochondria purified from spinal cords or livers of non transgenic rats (Figure 5A). Although a proportion of each of the recombinant SOD1s associated with both spinal cord and liver mitochondria (Figure 5D), accumulation of radio-labeled Ca^{2+} (presumably through the action of the mitochondrial calcium uniporter) into spinal cord or liver mitochondria was not affected by the addition of wild-type or mutant SOD1 (Figure 5C). On the other hand, VDAC1-mediated ADP accumulation into the same spinal cord or liver mitochondria was inhibited by both hSOD1^{G93A} and hSOD1^{G85R} mutants, but not hSOD1^{wt} (Figure 5B). This inhibition corresponded to a proportion of misfolded SOD1 associated with those mitochondria after incubation with either mutant, but not wild-type SOD1, as demonstrated by immunoprecipitation of intact mitochondria with the DSE2 antibody to misfolded SOD1 (Figure 5E). In contrast, wild-type SOD1 associated with the same mitochondria was not recognized by this misfolded SOD1 antibody (Figure 5E), consistent with its retention of normal folding and/or import into those mitochondria (Figure 5E).

Reduced VDAC1 Activity Diminishes Survival of Mutant SOD1^{G37R} Mice by Accelerating Disease Onset

Since we have established that (1) mutant SOD1 interacts directly with VDAC1 thereby inhibiting VDAC1 conductance (Figure 3), (2) spinal cord mitochondria from SOD1 mutant animals have progressive loss of ADP uptake, and (3) misfolded mutant SOD1 binds to normal mitochondria in vitro accompanied by selective loss of ADP conductance (Figure 5), we examined how reduced level and activity of VDAC1 affect disease course in SOD1^{G37R} mutant mice. To do this, we exploited mice heterozygous for disruption of the VDAC1 gene (producing what is effectively a null allele [Weeber et al., 2002]). These mice accumulate about half the normal level of VDAC1 protein (Figure 2S), while overall ADP conductance of spinal mitochondrial isolated from *VDAC1*$^{+/-}$ mice is reduced by ~25% (Figure 3S) relative to wild-type mice. After mating with SOD1^{G37R} mice, sex matched cohorts of mice and their littermates carrying the SOD1^{G37R} transgene and zero, one, or two active VDAC1 alleles were obtained and followed for disease onset, progression and survival. Measurement of ADP conductance of spinal mitochondria from *SOD1*^{G37R}/*VDAC1*$^{+/-}$ mice revealed a reduction to a level comparable to that corresponding to complete deletion of VDAC1 (Figure 3S).

A simple and objective measure of disease onset and early disease progression was applied by initiation of weight loss, reflecting denervation-induced muscle atrophy. While timing of progression from onset through either early (Figure 6E) or late (Figure 6F) disease phases was only modestly affected by reduction of VDAC1 levels, disease onset (Figures 6A and 6D) and

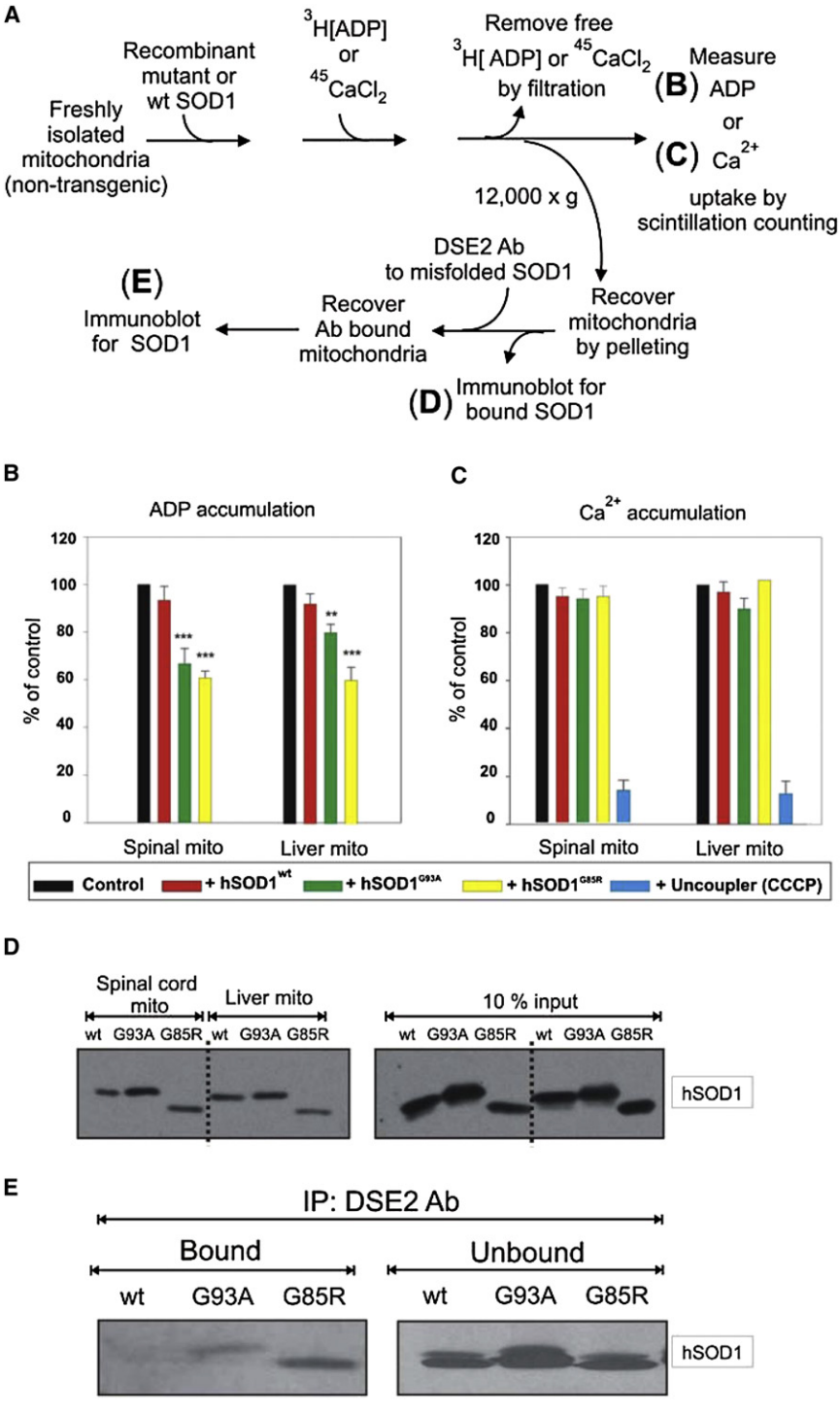

Figure 5. Mutant SOD1 Proteins Affect ADP but Not Ca^{2+} Accumulation into Mitochondria

(A) ADP or Ca^{2+} accumulation into isolated mitochondria was measured using a filter trap assay with radio-labeled $^{45}CaCl_2$ or [^{3}H]ADP. Mitochondria were isolated from fresh spinal cords and livers of nontransgenic rats.

(B) ADP and (C) Ca^{2+} accumulation were measured before and after the addition of 3 μM (50 μg/ml) hSOD1^{wt}, hSOD1^{G93A}, or hSOD1^{G85R} purified proteins. Student's t test was used and $p < 0.001$ (marked by three asterisks) and $p < 0.01$ (marked by two asterisks) were considered statistically significant. Values represent the means ± SEM of three independent experiments.

(D) Purified hSOD1^{wt}, hSOD1^{G93A}, or hSOD1^{G85R} were incubated with liver or spinal cord mitochondrial fractions purified from a nontransgenic rat for 20 min at 37°C. The samples were then washed three times and the mitochondrial pellet was subjected to immunoblot using an SOD1 antibody.

(E) Purified hSOD1^{wt}, hSOD1^{G93A}, or hSOD1^{G85R} was incubated for 20 min at 37°C with spinal cord mitochondria purified from nontransgenic rats. The samples were then washed three times and the mitochondrial pellet was subjected to immunoprecipitation using DSE2 (3H1) antibody, a monoclonal antibody only recognizing misfolded SOD1. The immunoprecipitates were immunoblotted using an SOD1 antibody.

progression to an early disease point (Figure 6B) were accelerated by 41 and 45 days, respectively, in *SOD1^{G37R}/VDAC1$^{+/-}$* mice (183 ± 22 and 230 ± 28 days) compared with their SOD1^{G37R} littermates (224 ± 19 and 275 ± 25 days). Moreover, age at which end stage disease was reached was also reduced by an average of 59 days (Figure 6C; *SOD1^{G37R}/VDAC1$^{+/-}$* mice [310 ± 42 days] compared with their SOD1^{G37R} littermates [369 ± 32 days]). A similar reduction in age of onset and life span was also observed for *SOD1^{G37R}/VDAC1$^{-/-}$* mice (Figure 4S), demonstrating that reduction in VDAC1 activity does affect SOD1 mutant-dependent pathogenesis, primarily by accelerating an early step in disease onset or spread.

DISCUSSION

We have demonstrated here in floated spinal cord mitochondria from mutant SOD1 expressing animals that both misfolded dismutase active or inactive SOD1 mutants bind directly and selectively to the cytoplasmically exposed face of VDAC1. Both dismutase active and dismutase inactive, but not wild-type, SOD1 binding to VDAC1 reduces channel conductance, as demonstrated for K^+ and Cl^- ions by electrophysiological recording and for ADP by inhibition of normal ADP accumulation into mitochondria. Channel conductance was not affected in liver mitochondria (where misfolded SOD1 does not accumulate). Mutant association and conductance inhibition is replicated in spinal cord mitochondria purified from mutant

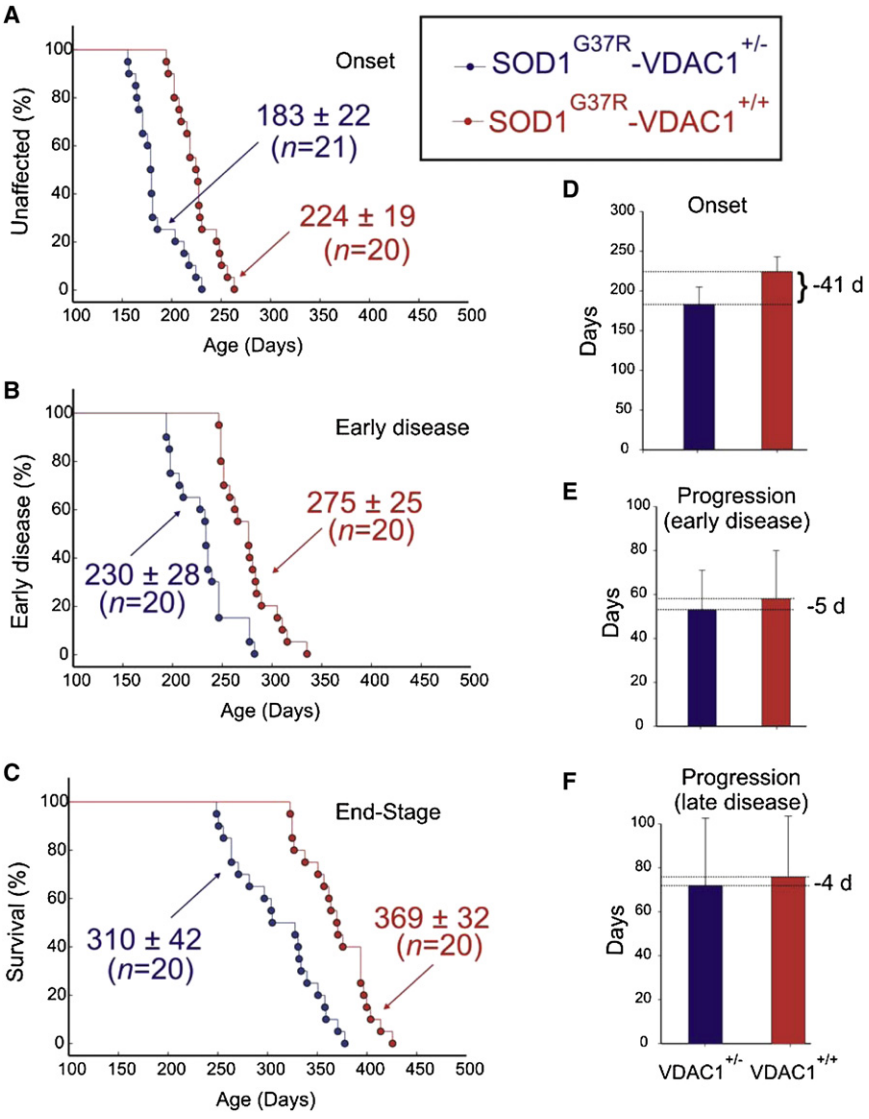

Figure 6. Reduction of VDAC1 Levels Accelerates Disease Onset and Diminishes Survival in the hSOD1^{G37R} Mouse Model of ALS

Ages of (A) disease onset (determined as the time when mice reached peak body weight), (B) early disease (determined as the time when mice lost 10% of maximal weight), and (C) disease end stage (determined as the time when the animal could not right itself within 20 s when placed on its side) of *SOD1^{G37R}-VDAC1$^{+/-}$* (blue) and *SOD1^{G37R}-VDAC1$^{+/+}$* littermates (red). Mean ages ± SD is provided.

(D, E, and F) Mean onset (D), mean duration of early disease (from onset to 10% weight loss, E) and mean duration of late disease (from 10% weight loss to end-stage, F). Error bars denote SD. See also Figure S4.

expressing animals beginning presymptomatically and increasing in severity during disease progression contemporaneous with increased accumulation of misfolded mutant SOD1. The clear implication from this is that only the misfolded portion of SOD1 is able to affect the channel, thereby partially blocking metabolite flux across the outer mitochondrial membrane. Reduced conductance by VDAC1 will decrease ATP synthesis, increase the ADP/ATP ratio in the cytosol and reduce membrane potential (as outlined in Figure 7). Chronic mitochondrial dysfunction can in turn drive generation of damaging reactive oxygen species that could drive further SOD1 misfolding through chemical damage to it, as has been previously documented selectively in spinal cords from mutant SOD1 animals (Liu et al., 2004; Vande Velde et al., 2008). Thus, our evidence demonstrates that reduced VDAC1 conductance, and correspondingly reduced respiration rate (Lemasters and Holmuhamedov, 2006), are direct components of intracellular damage from mutant SOD1.

Moreover, not only does mutant SOD1 lower VDAC1-dependent ADP conductance by half as much as does complete VDAC1 deletion (Figure 3S), further reduction in conductance (by VDAC1 gene inactivation) significantly accelerates disease onset (but not progression), reducing survival by more than two months for both VDAC1 heterozygous and homozygous mice. Intracellular targets for SOD1 damage beyond VDAC1 have been proposed (Ilieva et al., 2009), including aberrant glutamate handling from delayed synaptic glutamate recovery by astrocytes (Rothstein et al., 1995), mutant damage in the extracellular space following aberrant cosecretion with chromogranin (Urushitani et al., 2006), endoplasmic reticulum stress from inhibition of the ERAD pathway by mutant SOD1 binding to the integral membrane protein derlin (Nishitoh et al., 2008), and excessive production by microglia of extracellular superoxide following mutant SOD1 binding to the small G protein Rac1 and its subsequent stimulation of NAPDH oxidase (Harraz et al., 2008). Moreover, it was recently proposed that misfolded SOD1 damage to mitochondria can induce morphological changes and cytochrome c release in the presence of Bcl-2 (Pedrini et al., 2010). To those hypotheses, we propose that the partial blockage of the VDAC1 channel by direct association with misfolded SOD1 would make motor neurons more vulnerable to any of these additional stresses derived either from mutant SOD1 acting within motor neurons, astrocytes, microglia, and possibly additional neighboring nonneuronal cells. Indeed, in the presence of reduced VDAC1 conductance such pathways must play roles in pathogenesis, as we have shown that mutant SOD1-mediated disease still ensues in VDAC1 null mice.

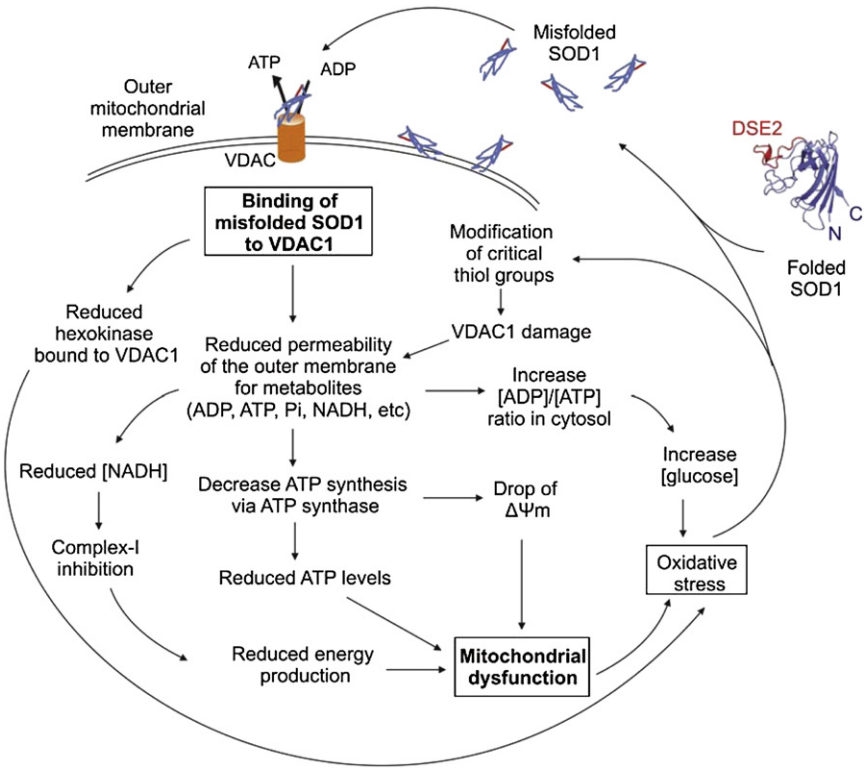

Figure 7. Effects of Misfolded SOD1 Binding to VDAC1

Model showing the effects of misfolded SOD1 binding to VDAC1. Misfolded SOD1 is proposed to inhibit VDAC1 conductance and suppress both uptake and release of mitochondrial metabolites.

This reduction in metabolites flux would result in reduced energy production and oxidative stress leading to mitochondrial dysfunction.

Surprisingly, in the absence of VDAC1, we have found a 60% residual ADP conductance which seems most likely to be contributed by compensatory VDACs or VDAC-like activity(ies). Although no other VDAC isoform is known to be overexpressed in VDAC1 null mice, VDAC2 has been shown to exist in two forms that differ in conductance and selectivity (Xu et al., 1999). It is plausible that in the absence of VDAC1, VDAC2 exists predominantly in a high conductance state, as a compensatory mechanism. This mechanism should now be tested by purifying VDAC2 from VDAC1 knockout mouse, and testing its channel properties in lipid bilayers.

The compromise in mutant SOD1-mediated VDAC1 conductance that we have found offers a mechanistic explanation for alteration in mitochondrial electron transfer chain complexes and the capacity to consume oxygen and synthesize ATP previously reported in one mutant SOD1 expressing mouse line (Jung et al., 2002; Kirkinezos et al., 2005; Mattiazzi et al., 2002). The recent report that association of $hSOD1^{G93A}$ and $hSOD1^{G85R}$ with motor neuron mitochondria reduces capacity of the electron transfer chain to limit Ca^{2+}-induced Ψm depolarization (Nguyen et al., 2009) is also fully compatible with altered adenine nucleotide transport across the outer mitochondrial membrane as the initiating deficit. So too is the report of reduced ability of mitochondria from $SOD1^{G93A}$ and $SOD1^{G85R}$ mice to survive repetitive Ca^{2+} addition (Damiano et al., 2006).

VDAC1 has been proposed to be the mediator for ROS release from the intermitochondrial spaces to the cytosol (Han et al., 2003; Madesh and Hajnóczky, 2001). Moreover, hexokinase (known to interact with VDAC1) has been shown in cell culture to decrease ROS release when overexpressed, thereby reducing intracellular levels of ROS (Ahmad et al., 2002; da-Silva et al., 2004). The relatively low level of hexokinase in spinal cord as compared to that in brain (Figure 1F) may therefore be a component of selective vulnerability. This is also consistent with the selective association of misfolded mutant SOD1 with VDAC1 on the cytoplasmic face of mitochondria from spinal cord, but not liver or brain. Although both tissues accumulate high levels of mutant SOD1 (Liu et al., 2004; Vande Velde et al., 2008), prior findings show that misfolded mutant SOD1 is bound to the cytoplasmic face of spinal cord mitochondria, while apparently imported into the intermembrane space of mitochondria from cortex of the same animals and not associated with liver mitochondria at all (Vande Velde et al., 2008). Another factor likely underlying the differences in mutant SOD1 association with mitochondria, and therefore potentially factors underlying selective vulnerability, is that mitochondria from different tissues (and which retain different functional properties) have different protein compositions (Bailey et al., 2007; Mootha et al., 2003), including hexokinase levels. This is accompanied by intrinsic differences in $O_2^{-\cdot}$ production, lipid peroxidation, DNA oxidation and Ca^{2+} accumulation capacity (Sullivan et al., 2004).

Our finding that VDAC1 is one of the targets for misfolded SOD1 within the nervous system raises substantial implications for the mechanism underlying premature degeneration and death of motor neurons. A variety of apoptotic stimuli are known to trigger cell death by modulation of VDAC1 (Abu-Hamad et al., 2008; Shoshan-Barmatz et al., 2006; Tsujimoto and Shimizu, 2002; Yagoda et al., 2007; Zaid et al., 2005; Zamzami and Kroemer, 2003; Zheng et al., 2004), implicating VDAC1 as a component of the apoptotic machinery. Although VDAC1 proteins have been reported to be dispensable for Ca^{2+} and oxidative stress-induced permeability transition pore (PTP) opening (Baines et al., 2007), siRNA-mediated reduction in VDAC1 has supported VDAC1 as an indispensable protein for endostatin-, cisplatin-, and selenite-induced oxidative stress induced PTP opening and apoptosis (Tajeddine et al., 2008; Tomasello et al., 2009; Yuan et al., 2008). Moreover, VDAC1 was recently shown to be involved in staurosporine- and

ceramide-induced cell death downstream of BAD and BCL-X_L (Roy et al., 2009) and curcumin induced apoptosis by cooperating with Bax in the release of AIF from mitochondria (Scharstuhl et al., 2009). Since VDAC1 is one of several targets for a cholesterol-like small molecule (TRO19622) that can protect motor neurons from SOD1 mutant-mediated death in culture and modestly delay disease onset in SOD1 mutant mice (Bordet et al., 2007), it now seems likely that its efficacy may be through direct effect on VDAC1.

Finally, it is well established that although motor neurons are the final targets in ALS, mutant damage within astrocytes and microglia contributes to driving rapid disease progression (Beers et al., 2006; Boillée et al., 2006a, 2006b; Clement et al., 2003; Yamanaka et al., 2008a, 2008b). In this context, we show here that little accumulation of misfolded SOD1 is found by disease onset, but it is preferentially within motor neurons. However, during disease progression a dramatic increase of misfolded SOD1 is observed accumulated in other cells as well and probably extracellularly. Interestingly, mitochondrial dysfunction(s) within mutant astrocytes has been reported to cause acute motor neuron death in astrocyte-motor neuron cocultures (Cassina et al., 2008) and astrocytes expressing mutant SOD1 have been reported to induce mitochondrial dysfunction within motor neurons (Bilsland et al., 2008). Coupling these findings with the appearance of aberrant mitochondria within motor neurons in multiple animal models of SOD1 mutant mediated ALS (Bendotti et al., 2001; Jaarsma et al., 2001; Kong and Xu, 1998; Wong et al., 1995) and the association of mutant SOD1 with mitochondria within affected tissues, we propose that misfolded SOD1 association directly with VDAC1 represents a primary event of damage within motor neurons.

EXPERIMENTAL PROCEDURES

Transgenic Rats and Mice

Transgenic rats expressing $hSOD1^{wt}$ (Chan et al., 1998), $hSOD1^{G93A}$ (Howland et al., 2002), and $hSOD1^{H46R}$ (Nagai et al., 2001) were as originally described. All animal procedures were consistent with the requirements of the Animal Care and Use Committee of the University of California.

Mice heterozygous for the mutant human $SOD1^{G37R}$ transgene ($LoxSOD1^{G37R}$) (Boillée et al., 2006b) were crossed with mice heterozygous for a VDAC1 gene disruption (Weeber et al., 2002). Mice were genotyped by PCR for the presence of the mutant SOD1 transgene (Williamson and Cleveland, 1999) and using a four-primer multiplex PCR for the presence of VDAC1 (Weeber et al., 2002), as previously described.

For survival experiments, $SOD1^{G37R}$, $VDAC1^{+/-}$ mice were always compared with their contemporaneously produced $SOD1^{G37R}$, $VDAC1^{+/+}$ littermates. Time of disease onset was retrospectively determined as the time when mice reached peak body weight, early disease was defined at the time when denervation-induced muscle atrophy had produced a 10% loss of maximal weight, and end-stage was determined by paralysis so severe that the animal could not right itself within 20 s when placed on its side, an endpoint frequently used for SOD1 mutant mice and one that was consistent with the requirements of the Animal Care and Use Committee of the University of California.

Subcellular Fractionation

Mitochondria were purified as previously described (Vande Velde et al., 2008). Tissues were homogenized on ice in 5 volumes of ice-cold homogenization buffer (HB) composed of 210 mM mannitol, 70 mM sucrose, 1 mM EDTA-(Tris) and 10 mM Tris-HCl (pH 7.2). Homogenates were centrifuged at 1,000 × g for 10 min. Supernatants were recovered, and pellets were washed with ½ volume HB and centrifuged at 1,000 × g. Supernatants were pooled and centrifuged at 12,000 × g for 15 min to yield a crude mitochondrial pellet. The supernatant was used to make cytosolic fractions by further centrifugation at 100,000 × g for 1 hr. The mitochondria were gently resuspended in HB and then adjusted to 1.204 g/ml Optiprep (iodixanol) and loaded on the bottom of a polycarbonate tube. Mitochondria were overlaid with an equal volume of 1.175 g/ml and 1.079 g/ml Optiprep and centrifuged at 50,000 × g for 4 hr (SW-55; Beckman). Mitochondria were collected at the 1.079/1.175 g/ml interface and washed once to remove the Optiprep. Optiprep stock solution was diluted in 250 mM sucrose, 120 mM Tris-HCl (pH 7.4), 6 mM EDTA plus protease inhibitors.

For activity assays, spinal cords were homogenized in 5 volumes of ice-cold homogenization buffer (HB) on ice. Homogenates were centrifuged at 1,000 × g for 5 min. Supernatants were recovered and centrifuged again at 1,000 × g for 5 min. Supernatants were centrifuged at 12,000 × g for 10 min to yield crude mitochondrial pellets. These mitochondria were gently resuspended in HB and then adjusted to 12% Optiprep (iodixanol) and centrifuged at 17,000 × g for 10 min (SW-55; Beckman). The majority of the myelin (at the top of the sample) was removed and the mitochondria were washed once with HB (without EDTA) to remove the Optiprep.

Liver was homogenized in 5 volumes of ice-cold homogenization buffer (HB) on ice. Homogenates were centrifuged at 1,000 × g for 5 min. Supernatants were recovered, and centrifuged again at 1,000 × g for 5 min. Supernatant was centrifuged at 12,000 × g for 10 min to yield a crude mitochondrial pellet. These mitochondria were resuspended in HB (without EDTA) and centrifuged again at 12,000 × g for 10 min. The pellet was resuspended in a small volume of HB without EDTA.

VDAC Channel Recording and Analysis

Reconstitution of VDAC into a planar lipid bilayer (PLB), single channel current recording, and data analysis were carried out as previously described (Gincel et al., 2001). Briefly, PLB were prepared from soybean asolectin dissolved in n-decane (50 mg/ml). Only PLB with a resistance greater than 100 GΩ, were used. Purified protein (about 1 ng) was added to the *cis* chamber. After one or a few channels were inserted into the PLB, the excess protein was removed by perfusion of the *cis* chamber with 20 volumes of a solution to prevent further incorporation. Currents were recorded under voltage-clamp using a Bilayer Clamp BC-525B amplifier (Warner Instrument Corp.). The currents were measured with respect to the *trans* side of the membrane (ground). The currents were low-pass, filtered at 1 kHz and digitized online using a Digidata 1200 interface board and pCLAMP 6 software (Axon Instruments, Inc.). Sigma Plot 6.0 scientific software (Jandel Scientific) was used for curve fitting. All experiments were performed at room temperature.

Please see Supplemental Information for the following experimental procedures: Protein Purification, Immunoprecipitation, DSE2 antibodies, Immunostaining, Ca^{2+} and ADP Accumulation by Mitochondria, and Immunoblotting.

SUPPLEMENTAL INFORMATION

Supplemental Information includes four figures and Supplemental Experimental Procedures and can be found with this article online at doi:10.1016/j.neuron.2010.07.019.

ACKNOWLEDGMENTS

We would like to thank Neil Cashman (University of British Columbia) and Amorfix Life Sciences (Vancouver) for generously providing us with DSE2 antibodies, William Craigen (Baylor College of Medicine) for VDAC1 knockout mice, and Larry Hayward (UMass Medical School) for wild type and mutant SOD1 baculovirus stock. This work has been supported by a grant from the NIH (R37 NS27036). A.I. has been supported by EMBO Long-Term Fellowship and by a postdoctoral fellowship from IsrALS. D.W.C. receives salary support from the Ludwig Institute for Cancer Research.

Accepted: July 22, 2010
Published: August 25, 2010

REFERENCES

Abu-Hamad, S., Sivan, S., and Shoshan-Barmatz, V. (2006). The expression level of the voltage-dependent anion channel controls life and death of the cell. Proc. Natl. Acad. Sci. USA *103*, 5787–5792.

Abu-Hamad, S., Zaid, H., Israelson, A., Nahon, E., and Shoshan-Barmatz, V. (2008). Hexokinase-I protection against apoptotic cell death is mediated via interaction with the voltage-dependent anion channel-1: mapping the site of binding. J. Biol. Chem. *283*, 13482–13490.

Abu-Hamad, S., Arbel, N., Calo, D., Arzoine, L., Israelson, A., Keinan, N., Ben-Romano, R., Friedman, O., and Shoshan-Barmatz, V. (2009). The VDAC1 N-terminus is essential both for apoptosis and the protective effect of anti-apoptotic proteins. J. Cell Sci. *122*, 1906–1916.

Ahmad, A., Ahmad, S., Schneider, B.K., Allen, C.B., Chang, L.Y., and White, C.W. (2002). Elevated expression of hexokinase II protects human lung epithelial-like A549 cells against oxidative injury. Am. J. Physiol. *283*, L573–L584.

Arbel, N., and Shoshan-Barmatz, V. (2010). Voltage-dependent anion channel 1-based peptides interact with Bcl-2 to prevent antiapoptotic activity. J. Biol. Chem. *285*, 6053–6062.

Azoulay-Zohar, H., Israelson, A., Abu-Hamad, S., and Shoshan-Barmatz, V. (2004). In self-defence: hexokinase promotes voltage-dependent anion channel closure and prevents mitochondria-mediated apoptotic cell death. Biochem. J. *377*, 347–355.

Bailey, A.O., Miller, T.M., Dong, M.Q., Vande Velde, C., Cleveland, D.W., and Yates, J.R. (2007). RCADiA: simple automation platform for comparative multidimensional protein identification technology. Anal. Chem. *79*, 6410–6418.

Baines, C.P., Kaiser, R.A., Sheiko, T., Craigen, W.J., and Molkentin, J.D. (2007). Voltage-dependent anion channels are dispensable for mitochondrial-dependent cell death. Nat. Cell Biol. *9*, 550–555.

Beers, D.R., Henkel, J.S., Xiao, Q., Zhao, W., Wang, J., Yen, A.A., Siklos, L., McKercher, S.R., and Appel, S.H. (2006). Wild-type microglia extend survival in PU.1 knockout mice with familial amyotrophic lateral sclerosis. Proc. Natl. Acad. Sci. USA *103*, 16021–16026.

Bendotti, C., Calvaresi, N., Chiveri, L., Prelle, A., Moggio, M., Braga, M., Silani, V., and De Biasi, S. (2001). Early vacuolization and mitochondrial damage in motor neurons of FALS mice are not associated with apoptosis or with changes in cytochrome oxidase histochemical reactivity. J. Neurol. Sci. *191*, 25–33.

Benz, R. (1994). Permeation of hydrophilic solutes through mitochondrial outer membranes: review on mitochondrial porins. Biochim. Biophys. Acta *1197*, 167–196.

Bergemalm, D., Jonsson, P.A., Graffmo, K.S., Andersen, P.M., Brännström, T., Rehnmark, A., and Marklund, S.L. (2006). Overloading of stable and exclusion of unstable human superoxide dismutase-1 variants in mitochondria of murine amyotrophic lateral sclerosis models. J. Neurosci. *26*, 4147–4154.

Bilsland, L.G., Nirmalananthan, N., Yip, J., Greensmith, L., and Duchen, M.R. (2008). Expression of mutant SOD1 in astrocytes induces functional deficits in motoneuron mitochondria. J. Neurochem. *107*, 1271–1283.

Boillée, S., Vande Velde, C., and Cleveland, D.W. (2006a). ALS: a disease of motor neurons and their nonneuronal neighbors. Neuron *52*, 39–59.

Boillée, S., Yamanaka, K., Lobsiger, C.S., Copeland, N.G., Jenkins, N.A., Kassiotis, G., Kollias, G., and Cleveland, D.W. (2006b). Onset and progression in inherited ALS determined by motor neurons and microglia. Science *312*, 1389–1392.

Bordet, T., Buisson, B., Michaud, M., Drouot, C., Galéa, P., Delaage, P., Akentieva, N.P., Evers, A.S., Covey, D.F., Ostuni, M.A., et al. (2007). Identification and characterization of cholest-4-en-3-one, oxime (TRO19622), a novel drug candidate for amyotrophic lateral sclerosis. J. Pharmacol. Exp. Ther. *322*, 709–720.

Bruijn, L.I., Becher, M.W., Lee, M.K., Anderson, K.L., Jenkins, N.A., Copeland, N.G., Sisodia, S.S., Rothstein, J.D., Borchelt, D.R., Price, D.L., and Cleveland, D.W. (1997). ALS-linked SOD1 mutant G85R mediates damage to astrocytes and promotes rapidly progressive disease with SOD1-containing inclusions. Neuron *18*, 327–338.

Cashman, N.R., and Caughey, B. (2004). Prion diseases—close to effective therapy? Nat. Rev. Drug Discov. *3*, 874–884.

Cassina, P., Cassina, A., Pehar, M., Castellanos, R., Gandelman, M., de León, A., Robinson, K.M., Mason, R.P., Beckman, J.S., Barbeito, L., and Radi, R. (2008). Mitochondrial dysfunction in SOD1G93A-bearing astrocytes promotes motor neuron degeneration: prevention by mitochondrial-targeted antioxidants. J. Neurosci. *28*, 4115–4122.

Chan, P.H., Kawase, M., Murakami, K., Chen, S.F., Li, Y., Calagui, B., Reola, L., Carlson, E., and Epstein, C.J. (1998). Overexpression of SOD1 in transgenic rats protects vulnerable neurons against ischemic damage after global cerebral ischemia and reperfusion. J. Neurosci. *18*, 8292–8299.

Clement, A.M., Nguyen, M.D., Roberts, E.A., Garcia, M.L., Boillée, S., Rule, M., McMahon, A.P., Doucette, W., Siwek, D., Ferrante, R.J., et al. (2003). Wild-type nonneuronal cells extend survival of SOD1 mutant motor neurons in ALS mice. Science *302*, 113–117.

Cleveland, D.W., and Rothstein, J.D. (2001). From Charcot to Lou Gehrig: deciphering selective motor neuron death in ALS. Nat. Rev. Neurosci. *2*, 806–819.

Colombini, M. (2004). VDAC: the channel at the interface between mitochondria and the cytosol. Mol. Cell. Biochem. *256-257*, 107–115.

da-Silva, W.S., Gómez-Puyou, A., de Gómez-Puyou, M.T., Moreno-Sanchez, R., De Felice, F.G., de Meis, L., Oliveira, M.F., and Galina, A. (2004). Mitochondrial bound hexokinase activity as a preventive antioxidant defense: steady-state ADP formation as a regulatory mechanism of membrane potential and reactive oxygen species generation in mitochondria. J. Biol. Chem. *279*, 39846–39855.

Dal Canto, M.C., and Gurney, M.E. (1994). Development of central nervous system pathology in a murine transgenic model of human amyotrophic lateral sclerosis. Am. J. Pathol. *145*, 1271–1279.

Damiano, M., Starkov, A.A., Petri, S., Kipiani, K., Kiaei, M., Mattiazzi, M., Flint Beal, M., and Manfredi, G. (2006). Neural mitochondrial Ca2+ capacity impairment precedes the onset of motor symptoms in G93A Cu/Zn-superoxide dismutase mutant mice. J. Neurochem. *96*, 1349–1361.

Deng, H.X., Shi, Y., Furukawa, Y., Zhai, H., Fu, R., Liu, E., Gorrie, G.H., Khan, M.S., Hung, W.Y., Bigio, E.H., et al. (2006). Conversion to the amyotrophic lateral sclerosis phenotype is associated with intermolecular linked insoluble aggregates of SOD1 in mitochondria. Proc. Natl. Acad. Sci. USA *103*, 7142–7147.

Dupuis, L., di Scala, F., Rene, F., de Tapia, M., Oudart, H., Pradat, P.F., Meininger, V., and Loeffler, J.P. (2003). Up-regulation of mitochondrial uncoupling protein 3 reveals an early muscular metabolic defect in amyotrophic lateral sclerosis. FASEB J. *17*, 2091–2093.

Echaniz-Laguna, A., Zoll, J., Ribera, F., Tranchant, C., Warter, J.M., Lonsdorfer, J., and Lampert, E. (2002). Mitochondrial respiratory chain function in skeletal muscle of ALS patients. Ann. Neurol. *52*, 623–627.

Geisler, S., Holmström, K.M., Skujat, D., Fiesel, F.C., Rothfuss, O.C., Kahle, P.J., and Springer, W. (2010). PINK1/Parkin-mediated mitophagy is dependent on VDAC1 and p62/SQSTM1. Nat. Cell Biol. *12*, 119–131.

Gincel, D., Zaid, H., and Shoshan-Barmatz, V. (2001). Calcium binding and translocation by the voltage-dependent anion channel: a possible regulatory mechanism in mitochondrial function. Biochem. J. *358*, 147–155.

Han, D., Antunes, F., Canali, R., Rettori, D., and Cadenas, E. (2003). Voltage-dependent anion channels control the release of the superoxide anion from mitochondria to cytosol. J. Biol. Chem. *278*, 5557–5563.

Harraz, M.M., Marden, J.J., Zhou, W., Zhang, Y., Williams, A., Sharov, V.S., Nelson, K., Luo, M., Paulson, H., Schöneich, C., and Engelhardt, J.F. (2008). SOD1 mutations disrupt redox-sensitive Rac regulation of NADPH oxidase in a familial ALS model. J. Clin. Invest. *118*, 659–670.

Hayward, L.J., Rodriguez, J.A., Kim, J.W., Tiwari, A., Goto, J.J., Cabelli, D.E., Valentine, J.S., and Brown, R.H., Jr. (2002). Decreased metallation and activity in subsets of mutant superoxide dismutases associated with familial amyotrophic lateral sclerosis. J. Biol. Chem. *277*, 15923–15931.

Higgins, C.M., Jung, C., and Xu, Z. (2003). ALS-associated mutant SOD1G93A causes mitochondrial vacuolation by expansion of the intermembrane space

and by involvement of SOD1 aggregation and peroxisomes. BMC Neurosci. *4*, 16.

Hirano, A., Donnenfeld, H., Sasaki, S., and Nakano, I. (1984a). Fine structural observations of neurofilamentous changes in amyotrophic lateral sclerosis. J. Neuropathol. Exp. Neurol. *43*, 461–470.

Hirano, A., Nakano, I., Kurland, L.T., Mulder, D.W., Holley, P.W., and Saccomanno, G. (1984b). Fine structural study of neurofibrillary changes in a family with amyotrophic lateral sclerosis. J. Neuropathol. Exp. Neurol. *43*, 471–480.

Hodge, T., and Colombini, M. (1997). Regulation of metabolite flux through voltage-gating of VDAC channels. J. Membr. Biol. *157*, 271–279.

Howland, D.S., Liu, J., She, Y., Goad, B., Maragakis, N.J., Kim, B., Erickson, J., Kulik, J., DeVito, L., Psaltis, G., et al. (2002). Focal loss of the glutamate transporter EAAT2 in a transgenic rat model of SOD1 mutant-mediated amyotrophic lateral sclerosis (ALS). Proc. Natl. Acad. Sci. USA *99*, 1604–1609.

Ilieva, H., Polymenidou, M., and Cleveland, D.W. (2009). Non-cell autonomous toxicity in neurodegenerative disorders: ALS and beyond. J. Cell Biol. *187*, 761–772.

Israelson, A., Arzoine, L., Abu-hamad, S., Khodorkovsky, V., and Shoshan-Barmatz, V. (2005). A photoactivable probe for calcium binding proteins. Chem. Biol. *12*, 1169–1178.

Jaarsma, D., Rognoni, F., van Duijn, W., Verspaget, H.W., Haasdijk, E.D., and Holstege, J.C. (2001). CuZn superoxide dismutase (SOD1) accumulates in vacuolated mitochondria in transgenic mice expressing amyotrophic lateral sclerosis-linked SOD1 mutations. Acta Neuropathol. *102*, 293–305.

Jung, C., Higgins, C.M., and Xu, Z. (2002). Mitochondrial electron transport chain complex dysfunction in a transgenic mouse model for amyotrophic lateral sclerosis. J. Neurochem. *83*, 535–545.

Kirkinezos, I.G., Bacman, S.R., Hernandez, D., Oca-Cossio, J., Arias, L.J., Perez-Pinzon, M.A., Bradley, W.G., and Moraes, C.T. (2005). Cytochrome c association with the inner mitochondrial membrane is impaired in the CNS of G93A-SOD1 mice. J. Neurosci. *25*, 164–172.

Kong, J., and Xu, Z. (1998). Massive mitochondrial degeneration in motor neurons triggers the onset of amyotrophic lateral sclerosis in mice expressing a mutant SOD1. J. Neurosci. *18*, 3241–3250.

Lemasters, J.J., and Holmuhamedov, E. (2006). Voltage-dependent anion channel (VDAC) as mitochondrial governator—thinking outside the box. Biochim. Biophys. Acta *1762*, 181–190.

Liu, J., Lillo, C., Jonsson, P.A., Vande Velde, C., Ward, C.M., Miller, T.M., Subramaniam, J.R., Rothstein, J.D., Marklund, S., Andersen, P.M., et al. (2004). Toxicity of familial ALS-linked SOD1 mutants from selective recruitment to spinal mitochondria. Neuron *43*, 5–17.

Madesh, M., and Hajnóczky, G. (2001). VDAC-dependent permeabilization of the outer mitochondrial membrane by superoxide induces rapid and massive cytochrome c release. J. Cell Biol. *155*, 1003–1015.

Mattiazzi, M., D'Aurelio, M., Gajewski, C.D., Martushova, K., Kiaei, M., Beal, M.F., and Manfredi, G. (2002). Mutated human SOD1 causes dysfunction of oxidative phosphorylation in mitochondria of transgenic mice. J. Biol. Chem. *277*, 29626–29633.

Mootha, V.K., Bunkenborg, J., Olsen, J.V., Hjerrild, M., Wisniewski, J.R., Stahl, E., Bolouri, M.S., Ray, H.N., Sihag, S., Kamal, M., et al. (2003). Integrated analysis of protein composition, tissue diversity, and gene regulation in mouse mitochondria. Cell *115*, 629–640.

Mulder, D.W., Kurland, L.T., Offord, K.P., and Beard, C.M. (1986). Familial adult motor neuron disease: amyotrophic lateral sclerosis. Neurology *36*, 511–517.

Nagai, M., Aoki, M., Miyoshi, I., Kato, M., Pasinelli, P., Kasai, N., Brown, R.H., Jr., and Itoyama, Y. (2001). Rats expressing human cytosolic copper-zinc superoxide dismutase transgenes with amyotrophic lateral sclerosis: associated mutations develop motor neuron disease. J. Neurosci. *21*, 9246–9254.

Nguyen, K.T., García-Chacón, L.E., Barrett, J.N., Barrett, E.F., and David, G. (2009). The Psi(m) depolarization that accompanies mitochondrial Ca2+ uptake is greater in mutant SOD1 than in wild-type mouse motor terminals. Proc. Natl. Acad. Sci. USA *106*, 2007–2011.

Nishitoh, H., Kadowaki, H., Nagai, A., Maruyama, T., Yokota, T., Fukutomi, H., Noguchi, T., Matsuzawa, A., Takeda, K., and Ichijo, H. (2008). ALS-linked mutant SOD1 induces ER stress- and ASK1-dependent motor neuron death by targeting Derlin-1. Genes Dev. *22*, 1451–1464.

Paramithiotis, E., Pinard, M., Lawton, T., LaBoissiere, S., Leathers, V.L., Zou, W.Q., Estey, L.A., Lamontagne, J., Lehto, M.T., Kondejewski, L.H., et al. (2003). A prion protein epitope selective for the pathologically misfolded conformation. Nat. Med. *9*, 893–899.

Pedrini, S., Sau, D., Guareschi, S., Bogush, M., Brown, R.H., Jr., Naniche, N., Kia, A., Trotti, D., and Pasinelli, P. (2010). ALS-linked mutant SOD1 damages mitochondria by promoting conformational changes in Bcl-2. Hum. Mol. Genet. *19*, 2974–2986.

Rakhit, R., Robertson, J., Vande Velde, C., Horne, P., Ruth, D.M., Griffin, J., Cleveland, D.W., Cashman, N.R., and Chakrabartty, A. (2007). An immunological epitope selective for pathological monomer-misfolded SOD1 in ALS. Nat. Med. *13*, 754–759.

Rosen, D.R., Siddique, T., Patterson, D., Figlewicz, D.A., Sapp, P., Hentati, A., Donaldson, D., Goto, J., O'Regan, J.P., Deng, H.X., et al. (1993). Mutations in Cu/Zn superoxide dismutase gene are associated with familial amyotrophic lateral sclerosis. Nature *362*, 59–62.

Rostovtseva, T.K., and Bezrukov, S.M. (1998). ATP transport through a single mitochondrial channel, VDAC, studied by current fluctuation analysis. Biophys. J. *74*, 2365–2373.

Rostovtseva, T., and Colombini, M. (1997). VDAC channels mediate and gate the flow of ATP: implications for the regulation of mitochondrial function. Biophys. J. *72*, 1954–1962.

Rothstein, J.D., Van Kammen, M., Levey, A.I., Martin, L.J., and Kuncl, R.W. (1995). Selective loss of glial glutamate transporter GLT-1 in amyotrophic lateral sclerosis. Ann. Neurol. *38*, 73–84.

Roy, S.S., Madesh, M., Davies, E., Antonsson, B., Danial, N., and Hajnóczky, G. (2009). Bad targets the permeability transition pore independent of Bax or Bak to switch between Ca^{2+}-dependent cell survival and death. Mol. Cell *33*, 377–388.

Sasaki, S., and Iwata, M. (1996). Dendritic synapses of anterior horn neurons in amyotrophic lateral sclerosis: an ultrastructural study. Acta Neuropathol. *91*, 278–283.

Sasaki, S., and Iwata, M. (2007). Mitochondrial alterations in the spinal cord of patients with sporadic amyotrophic lateral sclerosis. J. Neuropathol. Exp. Neurol. *66*, 10–16.

Scharstuhl, A., Mutsaers, H.A., Pennings, S.W., Russel, F.G., and Wagener, F.A. (2009). Involvement of VDAC, Bax and ceramides in the efflux of AIF from mitochondria during curcumin-induced apoptosis. PLoS ONE *4*, e6688. 10.1371/journal.pone.0006688.

Shimizu, S., Narita, M., and Tsujimoto, Y. (1999). Bcl-2 family proteins regulate the release of apoptogenic cytochrome c by the mitochondrial channel VDAC. Nature *399*, 483–487.

Shoshan-Barmatz, V., Israelson, A., Brdiczka, D., and Sheu, S.S. (2006). The voltage-dependent anion channel (VDAC): function in intracellular signalling, cell life and cell death. Curr. Pharm. Des. *12*, 2249–2270.

Shoshan-Barmatz, V., Keinan, N., and Zaid, H. (2008). Uncovering the role of VDAC in the regulation of cell life and death. J. Bioenerg. Biomembr. *40*, 183–191.

Sullivan, P.G., Rabchevsky, A.G., Keller, J.N., Lovell, M., Sodhi, A., Hart, R.P., and Scheff, S.W. (2004). Intrinsic differences in brain and spinal cord mitochondria: Implication for therapeutic interventions. J. Comp. Neurol. *474*, 524–534.

Tajeddine, N., Galluzzi, L., Kepp, O., Hangen, E., Morselli, E., Senovilla, L., Araujo, N., Pinna, G., Larochette, N., Zamzami, N., et al. (2008). Hierarchical involvement of Bak, VDAC1 and Bax in cisplatin-induced cell death. Oncogene *27*, 4221–4232.

Tomasello, F., Messina, A., Lartigue, L., Schembri, L., Medina, C., Reina, S., Thoraval, D., Crouzet, M., Ichas, F., De Pinto, V., and De Giorgi, F. (2009). Outer membrane VDAC1 controls permeability transition of the inner mitochondrial

membrane in cellulo during stress-induced apoptosis. Cell Res. *19*, 1363–1376.

Tsujimoto, Y., and Shimizu, S. (2002). The voltage-dependent anion channel: an essential player in apoptosis. Biochimie *84*, 187–193.

Urushitani, M., Sik, A., Sakurai, T., Nukina, N., Takahashi, R., and Julien, J.P. (2006). Chromogranin-mediated secretion of mutant superoxide dismutase proteins linked to amyotrophic lateral sclerosis. Nat. Neurosci. *9*, 108–118.

Urushitani, M., Ezzi, S.A., and Julien, J.P. (2007). Therapeutic effects of immunization with mutant superoxide dismutase in mice models of amyotrophic lateral sclerosis. Proc. Natl. Acad. Sci. USA *104*, 2495–2500.

Vande Velde, C., Miller, T.M., Cashman, N.R., and Cleveland, D.W. (2008). Selective association of misfolded ALS-linked mutant SOD1 with the cytoplasmic face of mitochondria. Proc. Natl. Acad. Sci. USA *105*, 4022–4027.

Vielhaber, S., Winkler, K., Kirches, E., Kunz, D., Büchner, M., Feistner, H., Elger, C.E., Ludolph, A.C., Riepe, M.W., and Kunz, W.S. (1999). Visualization of defective mitochondrial function in skeletal muscle fibers of patients with sporadic amyotrophic lateral sclerosis. J. Neurol. Sci. *169*, 133–139.

Vijayvergiya, C., Beal, M.F., Buck, J., and Manfredi, G. (2005). Mutant superoxide dismutase 1 forms aggregates in the brain mitochondrial matrix of amyotrophic lateral sclerosis mice. J. Neurosci. *25*, 2463–2470.

Weeber, E.J., Levy, M., Sampson, M.J., Anflous, K., Armstrong, D.L., Brown, S.E., Sweatt, J.D., and Craigen, W.J. (2002). The role of mitochondrial porins and the permeability transition pore in learning and synaptic plasticity. J. Biol. Chem. *277*, 18891–18897.

Wiedemann, F.R., Manfredi, G., Mawrin, C., Beal, M.F., and Schon, E.A. (2002). Mitochondrial DNA and respiratory chain function in spinal cords of ALS patients. J. Neurochem. *80*, 616–625.

Williamson, T.L., and Cleveland, D.W. (1999). Slowing of axonal transport is a very early event in the toxicity of ALS-linked SOD1 mutants to motor neurons. Nat. Neurosci. *2*, 50–56.

Wong, P.C., Pardo, C.A., Borchelt, D.R., Lee, M.K., Copeland, N.G., Jenkins, N.A., Sisodia, S.S., Cleveland, D.W., and Price, D.L. (1995). An adverse property of a familial ALS-linked SOD1 mutation causes motor neuron disease characterized by vacuolar degeneration of mitochondria. Neuron *14*, 1105–1116.

Xu, X., Decker, W., Sampson, M.J., Craigen, W.J., and Colombini, M. (1999). Mouse VDAC isoforms expressed in yeast: channel properties and their roles in mitochondrial outer membrane permeability. J. Membr. Biol. *170*, 89–102.

Yagoda, N., von Rechenberg, M., Zaganjor, E., Bauer, A.J., Yang, W.S., Fridman, D.J., Wolpaw, A.J., Smukste, I., Peltier, J.M., Boniface, J.J., et al. (2007). RAS-RAF-MEK-dependent oxidative cell death involving voltage-dependent anion channels. Nature *447*, 864–868.

Yamamoto, T., Yamada, A., Watanabe, M., Yoshimura, Y., Yamazaki, N., Yoshimura, Y., Yamauchi, T., Kataoka, M., Nagata, T., Terada, H., and Shinohara, Y. (2006). VDAC1, having a shorter N-terminus than VDAC2 but showing the same migration in an SDS-polyacrylamide gel, is the predominant form expressed in mitochondria of various tissues. J. Proteome Res. *5*, 3336–3344.

Yamanaka, K., Boillee, S., Roberts, E.A., Garcia, M.L., McAlonis-Downes, M., Mikse, O.R., Cleveland, D.W., and Goldstein, L.S. (2008a). Mutant SOD1 in cell types other than motor neurons and oligodendrocytes accelerates onset of disease in ALS mice. Proc. Natl. Acad. Sci. USA *105*, 7594–7599.

Yamanaka, K., Chun, S.J., Boillee, S., Fujimori-Tonou, N., Yamashita, H., Gutmann, D.H., Takahashi, R., Misawa, H., and Cleveland, D.W. (2008b). Astrocytes as determinants of disease progression in inherited amyotrophic lateral sclerosis. Nat. Neurosci. *11*, 251–253.

Yuan, S., Fu, Y., Wang, X., Shi, H., Huang, Y., Song, X., Li, L., Song, N., and Luo, Y. (2008). Voltage-dependent anion channel 1 is involved in endostatin-induced endothelial cell apoptosis. FASEB J. *22*, 2809–2820.

Zaid, H., Abu-Hamad, S., Israelson, A., Nathan, I., and Shoshan-Barmatz, V. (2005). The voltage-dependent anion channel-1 modulates apoptotic cell death. Cell Death Differ. *12*, 751–760.

Zamzami, N., and Kroemer, G. (2003). Apoptosis: mitochondrial membrane permeabilization—the (w)hole story? Curr. Biol. *13*, R71–R73.

Zheng, Y., Shi, Y., Tian, C., Jiang, C., Jin, H., Chen, J., Almasan, A., Tang, H., and Chen, Q. (2004). Essential role of the voltage-dependent anion channel (VDAC) in mitochondrial permeability transition pore opening and cytochrome c release induced by arsenic trioxide. Oncogene *23*, 1239–1247.